

Donor and acceptor competitions in phosphorus-doped ZnO

F. X. Xiu, Z. Yang, L. J. Mandalapu, and J. L. Liu^{a)}

Quantum Structures Laboratory, Department of Electrical Engineering, University of California, Riverside, California 92521

(Received 21 December 2005; accepted 1 March 2006; published online 14 April 2006)

Phosphorus-doped ZnO films were grown by molecular-beam epitaxy with a GaP effusion cell as dopant source. Three growth regions were identified to obtain ZnO films with different conduction types. In the oxygen-extremely-rich region, phosphorus-doped ZnO films show *n*-type conduction with dominant donor-bound excitons (D^0X) in the low-temperature photoluminescence (PL) spectra. In the oxygen-rich region, a growth window was found to generate *p*-type ZnO films. The PL spectra show evident competitions between D^0X and acceptor-bound excitons (A^0X). In the stoichiometric and Zn-rich region, ZnO films are *n*-type with dominant D^0X emissions. Thus, phosphorus doping is amphoteric, having the tendency to form both donors and acceptors in ZnO.

© 2006 American Institute of Physics. [DOI: 10.1063/1.2194870]

In the progress of developing reliable and reproducible *p*-type ZnO for ZnO-based optoelectronic and spintronic applications,¹ group V element phosphorus is one of the promising candidates of materials having good *p*-type electrical properties, such as high carrier concentration, high mobility, and low resistivity.²⁻⁹ In addition, rectifying *I-V* behavior was observed for diode employing phosphorus-doped *p*-type ZnO with *n*-type materials, further confirming the *p*-type conduction by phosphorus doping.¹⁰⁻¹⁴ However, the reliability of phosphorus *p*-type doping is still problematic. Furthermore, the lack of understanding of phosphorus doping mechanism hinders the progress of reliably producing phosphorus-doped *p*-type ZnO. In this work, we report a systematic study on electrical and optical properties of phosphorus-doped ZnO films grown by molecular-beam epitaxy with a GaP effusion cell as phosphorus dopant source. Combining room-temperature (RT) Hall effect and low-temperature (LT) photoluminescence (PL) measurements, the nature of phosphorus doping is explored.

The phosphorus-doped ZnO films were grown on (01 $\bar{1}$ 2) *r*-plane sapphire substrates. Elemental zinc (5N) was evaporated with a LT effusion cell. The oxygen (5N) plasma was generated with a radio-frequency plasma source. All films were grown at 720 °C with oxygen flow rate of 6 SCCM (SCCM denotes cubic centimeter per minute at STP). The growth time varied from 3 to 8 h, resulting in different thicknesses, as shown in Table I. After growth, a postannealing process was performed at 800 °C for 20 min to activate phosphorus dopants. The detailed growth procedures are presented elsewhere.⁸ In this study, two sets of samples were prepared, as shown in Table I. In the first set of films (samples a-e), Zn cell temperatures were varied from 320 to 380 °C while the GaP cell temperature was fixed at 710 °C. The growth rate is plotted as a function of Zn cell temperatures in Fig. 1; three growth regions (I-III) were identified accordingly. In region I, the growth rate is extremely low due to insufficient Zn atoms; therefore this region is assigned as an oxygen-extremely-rich region. RT Hall effect measurements show that the films in this region have

strong *n*-type conduction with high electron concentrations of 9.6×10^{18} – 2.0×10^{19} cm⁻³. In region II, the growth rate increases rapidly with Zn cell temperatures. Since the growth rate is still limited by Zn cell temperatures, this region is assigned as an oxygen-rich condition. The Hall effect measurements yield ambiguous carrier type for the films grown with Zn cell temperatures of 340 and 360 °C (samples b and d). This result may arise from the strong compensation effect with equivalent concentrations of electrons and holes in these two samples. By mediating the Zn cell temperature as 350 °C (sample c), however, strong *p*-type conduction was obtained with a hole concentration of 1.2×10^{18} cm⁻³ and a mobility of 4.2 cm²/V s.⁸ Further increasing the Zn cell temperature beyond 360 °C causes the saturation of growth rate, which corresponds to the stoichiometric and Zn-rich condition (region III). The films in this region show *n*-type conduction with typical electron concentration of 2.3×10^{18} cm⁻³.

To further study the properties of *p*-type phosphorus-doped ZnO and achieve controllable hole concentrations, the second set of films was prepared by varying GaP cell temperatures from 680, 710, to 750 °C while keeping the Zn cell temperature at 350 °C (region II, samples f, c, and g, respectively). RT Hall effect measurements show that with GaP cell temperatures of 710 and 750 °C, the phosphorus-doped ZnO films exhibit strong *p*-type conduction. For example, the sample grown with GaP cell temperature of 750 °C (sample g) has the highest hole concentration of 6.0×10^{18} cm⁻³ and a mobility of 1.5 cm²/V s. But the film with GaP cell temperature of 680 °C (sample f) shows *n*-type conduction with an electron concentration of 7.8×10^{17} cm⁻³. These data suggest that an oxygen-rich condition and a high GaP cell temperature are necessary for producing *p*-type ZnO by phosphorus doping using a GaP effusion cell.

Second ion mass spectroscopy (SIMS) was performed on phosphorus-doped *p*-type ZnO films to examine the incorporation and concentration of phosphorus dopants using a Cameca 4f SIMS system. The SIMS depth profiles are shown in Fig. 2. For the GaP cell temperatures of 710 and 750 °C, phosphorus doping concentrations were obtained as 2.0×10^{18} and 8.0×10^{18} cm⁻³, respectively. Comparing these values with the hole concentrations of 1.2×10^{18} and 6.0×10^{18} cm⁻³ obtained from Hall effect measurements, it is

^{a)} Author to whom correspondence should be addressed; electronic mail: jianlin@ee.ucr.edu

TABLE I. Growth conditions and RT electrical properties of phosphorus-doped ZnO films.

Sample	Zn cell temperature (°C)	GaP cell temperature (°C)	Thickness (μm)	Conduction type	Carrier concentration (cm^{-3})	Mobility ($\text{cm}^2/\text{V s}$)
a	320	710	0.29	<i>n</i>	2.0×10^{19}	31.3
b	340	710	0.53	Ambiguous	N/A	N/A
c	350	710	0.40	<i>p</i>	1.2×10^{18}	4.2
d	360	710	0.55	Ambiguous	N/A	N/A
e	370	710	0.62	<i>n</i>	2.3×10^{18}	45.2
f	350	680	0.40	<i>n</i>	7.8×10^{17}	2.4
g	350	750	0.74	<i>p</i>	6.0×10^{18}	1.5

believed that phosphorus dopants were completely activated at the annealing temperature of 800 °C.

LT PL measurements were carried out to investigate the optical transitions in these films. A 325 nm He–Cd laser was used as the excitation source. Figures 3(a)–3(e) show the PL spectra at 8.5 K for the first set of phosphorus-doped ZnO films grown with different Zn cell temperatures: (a) $T_{\text{Zn}}=320$ °C (region I); [(b)–(d)] $T_{\text{Zn}}=340, 350,$ and 360 °C, respectively (region II); and (e) $T_{\text{Zn}}=370$ °C (region III). In the oxygen-extremely-rich condition [region I, Fig. 3(a)], the PL spectrum is dominated by a strong D^0X emission, which was widely observed in undoped,¹ nitrogen-doped,¹⁵ phosphorus-doped,³ and arsenic-doped¹⁶ ZnO films. Another emission is observed at 3.256 eV, which may be attributed to phosphorus doping. By increasing Zn cell temperature to 340 °C [region II, Fig. 3(b)], the features of PL spectrum remain nearly the same except for a stronger emission at 3.267 eV. The RT Hall effect measurements reveal an indeterminate carrier type for this sample. By increasing the Zn cell temperature to 350 °C [region II, Fig. 3(c)], however, D^0X and A^0X emissions simultaneously show up in the PL spectrum at 3.364 and 3.315 eV, respectively, with a relatively stronger A^0X than D^0X . Consistently, the Hall effect measurement shows strong *p*-type conduction for this sample. The coexistence of D^0X and A^0X in this spectrum indicates that there are competitions between donors and acceptors in this film. By further increasing the Zn cell temperature to 360 °C [region II, Fig. 3(d)], the spectrum shows a lower intensity of A^0X than D^0X . Correspondingly, the Hall effect measurement does not yield a clear *p*-type conduction, similar to the scenario of $T_{\text{Zn}}=340$ °C [region II,

Fig. 3(b)]. The emissions at 3.259 and 3.180 eV were clearly observed and identified as free electron to acceptor (FA) and donor-acceptor pair (DAP) transitions, respectively, in our previous study.⁸ Finally, raising the Zn cell temperature to 370 °C leads to a dominant D^0X emission at 3.361 eV and a phosphorus-related emission at 3.303 eV [region III, Fig. 3(e)]. The Hall effect measurement reveals *n*-type conduction for this sample. From the evolution of PL spectra and Hall data, it is concluded that there are competitions between D^0X and A^0X in phosphorus-doped ZnO films, and by varying the Zn cell temperatures, the intensities of D^0X and A^0X emissions can be well controlled. The final carrier type is determined by the competition results.

Figures 3(f), 3(c), and 3(g) show the PL spectra at 8.5 K for the second set of phosphorus-doped ZnO films grown with different GaP cell temperatures of 680, 710, and 750 °C, respectively. With a low GaP cell temperature of 680 °C [Fig. 3(f)], the film shows *n*-type conduction with a D^0X dominated PL spectrum, similar to the case in Fig. 3(e). By increasing GaP cell temperature to 710 °C [Fig. 3(c)], the film becomes *p*-type and the spectrum shows the coexistence of D^0X and A^0X with a stronger A^0X emission, as analyzed above. Further raising the GaP cell temperature to 750 °C [Fig. 3(g)] results in a completely A^0X dominated PL spectrum at 3.317 eV and a nearly-diminished D^0X at 3.360 eV. Accordingly, the Hall effect measurement shows much stronger *p*-type conduction with a high hole concentration of $6.0 \times 10^{18} \text{ cm}^{-3}$ and a mobility of $1.5 \text{ cm}^2/\text{V s}$. The dramatic change of PL spectra in the second set of samples further proves the existence of competitions between D^0X and A^0X in phosphorus-doped ZnO films.

The doping mechanism for phosphorus-doped ZnO remains unclear and sometimes controversial.^{4,6,7,17–24} Recent

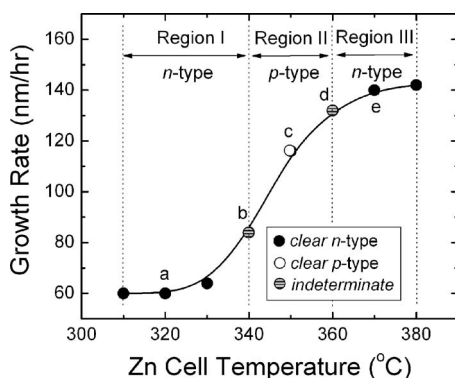


FIG. 1. Phosphorus-doped ZnO growth rate as a function of Zn cell temperature. Three regions were identified: Region I, oxygen-extremely-rich region (*n* type); region II, oxygen-rich region (*p* type); and region III, stoichiometric and Zn-rich region (*n* type). Samples a–e were also marked in this figure. The growth conditions can be found in Table I.

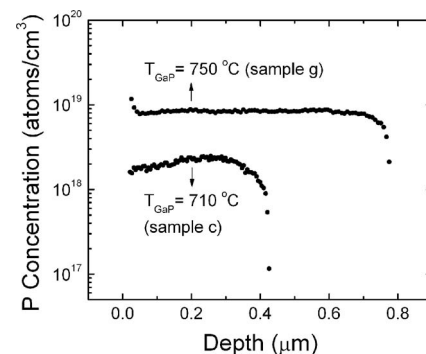


FIG. 2. The SIMS depth profiles for phosphorus-doped *p*-type ZnO films with $T_{\text{GaP}}=710$ and 750 °C. Phosphorus doping concentrations are obtained as 2.0×10^{18} and $8.0 \times 10^{18} \text{ cm}^{-3}$, respectively.

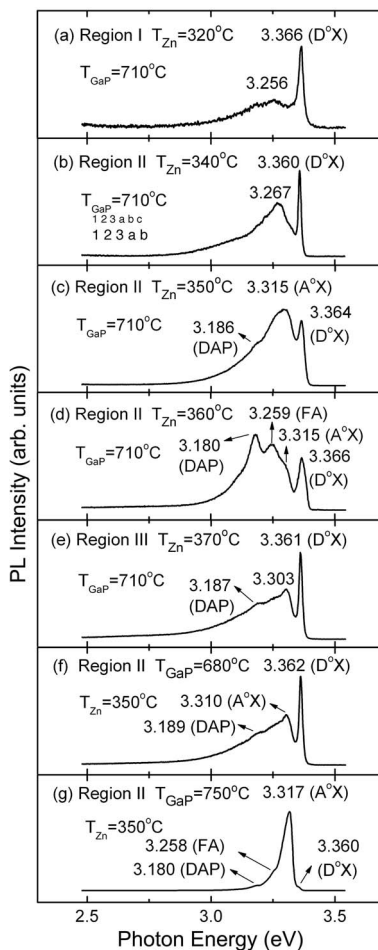


FIG. 3. PL spectra at 8.5 K for two sets of phosphorus-doped ZnO films. (a)–(g) are corresponding to samples a–g, as shown in Table I.

studies showed that the incorporation of phosphorus leads to a significant increase of electron concentration,^{5,18,20,21} suggesting that the formation of anti-site defects P_{Zn} and P^{+3-} , P^{+5-} , or P^{-3} -related complex could be the origin of shallow donors in phosphorus-doped *n*-type ZnO.^{20–22} Consistently, our results show that, in the oxygen-extremely-rich condition, the phosphorus-doped ZnO films become very conductive with electron concentrations up to $2.0 \times 10^{19} \text{ cm}^{-3}$. In the oxygen-rich condition, however, phosphorus-related A^0X emission starts to show up [Fig. 3(c)] and becomes much stronger by raising GaP cell temperature to 750 °C [Fig. 3(g)], which clearly indicates that high-density acceptors were incorporated into the films. Theoretical work has been done to understand the origin of *p*-type conduction by phosphorus doping.^{22–24} It was suggested that a possible shallow acceptor P_O^{-1} could be formed with an energy level of 0.49 eV above the valence band maximum.²² Experimentally, similar to As- and Sb-doped ZnO,^{3,25,26} the acceptor activation energy of phosphorus-doped ZnO films was shown to be much smaller than theoretical calculations, in the range of 127–180 meV.^{3,8} Nevertheless, the high hole concentration obtained in the present study indicates the formation of shallow phosphorus-related acceptors. It is also interesting to note that similar experimental results were obtained for pulsed laser deposition (PLD)-grown ZnO films using P_2O_5 as dopant source.⁶ Oxygen flow rates were varied from 20 to 200 mTorr and a narrow *p*-type growth window was found only with an oxygen flow rate of 150 mTorr. The

consistency of these experimental results confirmed that the phosphorus doping is of amphoteric character.

In summary, phosphorus-doped ZnO films were produced using a GaP cell as the phosphorus dopant source in a molecular-beam epitaxy system. Three growth regions were identified to generate ZnO films with different conduction types by systematically varying the Zn cell temperatures. A growth window was found to generate *p*-type ZnO films. The PL spectra clearly indicate the existence of competitions between D^0X and A^0X for the phosphorus-doped ZnO films, especially in the oxygen-rich region. This study suggests that to achieve reliable *p*-type ZnO by phosphorus doping, an adoption of oxygen-rich growth condition and high phosphorus incorporation during growth is needed to suppress/compensate the formation of donors. Hence, a high acceptor concentration could be achieved. Phosphorus doping mechanism is confirmed to be amphoteric. Depending on growth conditions, phosphorus-related donors and acceptors can be formed with different concentrations. The final carrier type is determined by the competition results.

This work was supported by DARPA/DMEA through the center for NanoScience and Innovation for Defense (CNID) under Award No. H94003-04-2-0404.

- ¹D. C. Look and B. Claflin, Phys. Status Solidi B **241**, 624 (2004).
- ²K. K. Kim, H. S. Kim, D. K. Hwang, J. H. Lim, and S. J. Park, Appl. Phys. Lett. **83**, 63 (2003).
- ³D. K. Hwang, H. S. Kim, J. H. Lim, J. Y. Oh, J. H. Yang, S. J. Park, K. K. Kim, D. C. Look, and Y. S. Park, Appl. Phys. Lett. **86**, 151917 (2005).
- ⁴F. G. Chen, Z. Z. Ye, W. Z. Xu, B. H. Zhao, L. P. Zhu, and J. G. Lv, J. Cryst. Growth **281**, 458 (2005).
- ⁵V. Vaithianathan, B. T. Lee, and S. S. Kim, J. Appl. Phys. **98**, 043519 (2005).
- ⁶Y. J. Li, Y. W. Heo, Y. Kwon, K. Ip, S. J. Pearton, and D. P. Norton, Appl. Phys. Lett. **87**, 072101 (2005).
- ⁷S. J. So and C. B. Park, J. Cryst. Growth **285**, 606 (2005).
- ⁸F. X. Xiu, Z. Yang, L. J. Mandalapu, J. L. Liu, and W. P. Beyermann, Appl. Phys. Lett. **88**, 052106 (2006).
- ⁹Y. Miao, Z. Z. Ye, W. Z. Xu, F. G. Chen, X. C. Zhou, B. G. Zhao, L. P. Zhu, and J. G. Lu, Appl. Surf. Sci. (unpublished).
- ¹⁰H. Yang, Y. Li, D. P. Norton, S. J. Pearton, S. Jung, F. Ren, and L. A. Boatner, Appl. Phys. Lett. **86**, 172103 (2005).
- ¹¹T. Aoki, Y. Hatanaka, and D. C. Look, Appl. Phys. Lett. **76**, 3257 (2000).
- ¹²K. H. Bang, D. K. Hwang, M. C. Park, Y. D. Ko, I. Yun, and J. M. Myoung, Appl. Surf. Sci. **210**, 177 (2003).
- ¹³Y. D. Ko, J. Jung, K. H. Bang, M. C. Park, K. S. Huh, J. M. Myoung, and I. Yun, Appl. Surf. Sci. **202**, 266 (2002).
- ¹⁴S. Jang, J. J. Chen, B. S. Kang, F. Ren, D. P. Norton, S. J. Pearton, J. Lopata, and W. S. Hobson, Appl. Phys. Lett. **87**, 222113 (2005).
- ¹⁵D. C. Look, D. C. Reynolds, C. W. Litton, R. L. Jones, D. B. Eason, and G. Cantwell, Appl. Phys. Lett. **81**, 1830 (2002).
- ¹⁶Y. R. Ryu, T. S. Lee, and H. W. White, Appl. Phys. Lett. **83**, 87 (2003).
- ¹⁷H. Tampo, H. Shibata, P. Fons, A. Yamada, K. Matsubara, K. Iwata, K. Tamura, H. Takasu, and S. Niki, J. Cryst. Growth **278**, 268 (2005).
- ¹⁸Z. Q. Chen, A. Kawasuso, Y. Xu, H. Naramoto, X. L. Yuan, T. Sekiguchi, R. Suzuki, and T. Ohdaira, J. Appl. Phys. **97**, 013528 (2005).
- ¹⁹Y. W. Heo, Y. W. Kwon, Y. Li, S. J. Pearton, and D. P. Norton, Appl. Phys. Lett. **84**, 3474 (2004).
- ²⁰Y. W. Heo, K. Ip, S. J. Park, S. J. Pearton, and D. P. Norton, Appl. Phys. A: Mater. Sci. Process. **78**, 53 (2004).
- ²¹Y. W. Heo, S. J. Park, K. Ip, S. J. Pearton, and D. P. Norton, Appl. Phys. Lett. **83**, 1128 (2003).
- ²²Z. G. Yu, H. Gong, and P. Wu, Appl. Phys. Lett. **86**, 212105 (2005).
- ²³Z. G. Yu, H. Gong, and P. Wu, Chem. Mater. **17**, 852 (2005).
- ²⁴C. H. Park, S. B. Zhang, and S. H. Wei, Phys. Rev. B **66**, 073202 (2002).
- ²⁵F. X. Xiu, Z. Yang, L. J. Mandalapu, D. T. Zhao, J. L. Liu, and W. P. Beyermann, Appl. Phys. Lett. **87**, 152101 (2005).
- ²⁶F. X. Xiu, Z. Yang, L. J. Mandalapu, D. T. Zhao, and J. L. Liu, Appl. Phys. Lett. **87**, 252102 (2005).